REVIEW OF SCIENTIFIC INSTRUMENTS VOLUME 72, NUMBER 2 FEBRUARY 2001

Ultrahigh vacuum cantilever magnetometry with standard size single crystal substrates

Th. Höpfl, D. Sander,[a] H. Höche, and J. Kirschner
Max-Planck-Institut für Mikrostrukturphysik, Weinberg 2, D-06120 Halle/Saale, Germany

(Received 21 July 2000; accepted for publication 20 November 2000)

A cantilever magnetometer is described that measures the magnetic moment of ferromagnetic films with submonolayer sensitivity. The magnetometer is incorporated into an ultrahigh vacuum chamber for sample preparation and *in situ* magnetometry. Standard size single crystals of 5 mm diameter and 2 mm thickness can be used, which are mounted on thin sheet metal. This composite sampleholder works as a cantilever when the bending is induced by the torque exerted by an external magnetic field on a monolayer ferromagnetic film deposited onto the single crystal substrate. We demonstrate the submonolayer sensitivity on Fe monolayers on Cu(100) in the thickness range from 2 to 68 monolayers. The sample holder is designed for internal calibration by passing a current through it and exploiting the well-known current induced magnetic moment.
© *2001 American Institute of Physics.* [DOI: 10.1063/1.1340560]

I. INTRODUCTION

For decades the magnetic properties of thin magnetic films have been investigated intensively.[1,2] However, the quantitative measurement of the magnetic moment of ferromagnetic monolayers under ultrahigh vacuum (UHV) conditions has faced considerable experimental obstacles. This is surprising in view of the numerous established techniques that have been successfully employed to measure the magnetic moment of *bulk* samples with a sensitivity comparable or even superior to one monolayer covering 10 mm.[2,3–8]

UHV compatible magnetometers that are designed to work with single crystal substrates covered with monolayer thin ferromagnetic films have been described. To name a few examples, the torsion oscillation magnetometer (TOM),[9] the alternating gradient magnetometer,[10] and the superconducting quantum interference device magnetometer[11,12] have demonstrated monolayer sensitivity. The cantilever bending magnetometer has been shown to give submonolayer sensitivity with the additional benefit of measuring film stress during film growth or magnetization processes.[13]

Weber *et al.*[13] introduced a cantilever magnetometer, that determined the magnetic moment of films in the monolayer thickness range under UHV conditions. In their work a thin substrate was clamped at one end and a ferromagnetic material was evaporated onto the front side. The use of a thin substrate has the advantage of measuring film stress from a curvature analysis of the substrate during film growth. However, this additional stress information requires the use of rather thin substrates which are difficult to make and expensive in the case of metal single crystals.

Under the influence of an external magnetic deflection field $\mathbf{B}_{\mathrm{defl}}$ a torque is acting on the magnetic moment $\mathbf{m}$ of the film

$$\mathbf{T}=\mathbf{m}\times\mathbf{B}_{\mathrm{defl}}. \tag{1}$$

This torque leads to a bending of the substrate which Weber *et al.* measured using a capacitance method.[13] Although the sensitivity of this technique is well below one monolayer and although the use of a thin substrate offers the additional possibility to measure forces in the film (film stress, magnetostrictive stress), this method shows decisive disadvantages: one needs very thin substrates, which are, e.g., in the case of Cu single crystals difficult to prepare and very sensitive against thermal and mechanical influences. Second, by using a capacitance method it is difficult to maintain easy access to the sample, which is necessary for some standard surface analysis techniques like low energy electron diffraction (LEED) or Auger electron spectroscopy (AES).

II. PRINCIPLE OF OPERATION

The basic idea of our technique is to apply a cantilever as a sample holder for single crystals with diameters of about 5 mm and a thickness of about 2 mm. These are standard dimensions for single crystals and the crystals are less expensive and much easier to handle and to prepare than the rather delicate single crystals used in former bending beam magnetometers.[13] The use of an optical deflection technique for the curvature measurements guarantees the free access to the sample. Figure 1 shows the principle of the magnetometer. On the free end of a cantilever, which is clamped on the other side, a compact single crystal is fixed and acts as the substrate for a ferromagnetic film. The film is magnetized by an external field $\mathbf{B}_{\mathrm{mag}}$. A deflection field $\mathbf{B}_{\mathrm{defl}}$ perpendicular to $\mathbf{B}_{\mathrm{mag}}$ causes a torque $\mathbf{T}$ which bends the cantilever.

This design allows a convenient use of standard single crystal substrates and it facilitates the experimental characterization of both substrate and film by LEED and AES.

A nonvanishing magnetic anisotropy is necessary for the torque measurements. In the limiting case of vanishing anisotropy the magnetization would align parallel to the result-

[a] Author to whom correspondence should be addressed; electronic mail: sander@mpi.halle.de

 © 2001 American Institute of Physics

Downloaded 20 Mar 2001 to 195.37.184.165. Redistribution subject to AIP copyright, see http://ojps.aip.org/rsio/rsicpyrts.html

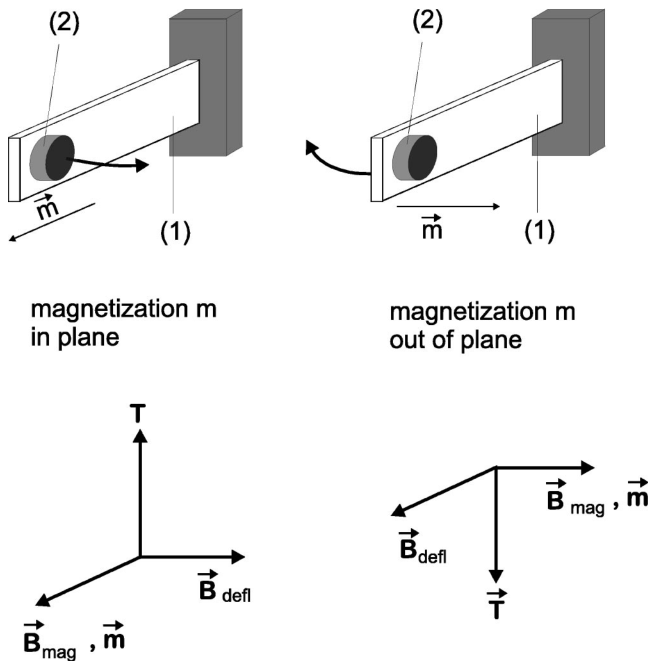

FIG. 1. Principle of the cantilever magnetometer. The cantilever (1) is fixed at one end. At the free end a single crystal (2) is mounted, which is used as a substrate for the ferromagnetic film. The deflection field $\mathbf{B}_{\mathrm{defl}}$ and the magnetizing field $\mathbf{B}_{\mathrm{mag}}$ are oriented differently for in-plane and out-of-plane magnetized films. The resulting torque $\mathbf{T}$ leads to a bending of the cantilever that is measured by a laser beam technique.

ing external magnetic field given by $(\mathbf{B}_{\mathrm{mag}}+\mathbf{B}_{\mathrm{defl}})$ and there would be no total torque acting on the cantilever, $\mathbf{T}_{\mathrm{total}}=\mathbf{m}\times(\mathbf{B}_{\mathrm{mag}}+\mathbf{B}_{\mathrm{defl}})=0$. In the case of a strong anisotropy one can distinguish between two geometries: Fig. 1(a) the easy axis of magnetization is in plane and parallel to the cantilever axis. The necessary torque is created by a deflection field parallel to the film normal. If the magnetization is oriented out of plane, Fig. 1(b), the deflection field is oriented parallel to the cantilever axis to create the bending torque.

If we assume, for simplicity, that the anisotropy is very strong then the magnetically induced torque will be proportional to the deflection field and the total magnetic moment of the film. Thus, a curvature analysis of the bent beam is capable of determining the total magnetic moment of the film. This is the idea of any cantilever magnetometer. If the anisotropy of the film is weak then the torque will be no longer proportional to $\mathbf{B}_{\mathrm{defl}}$ and the magnetization $\mathbf{m}$ will rotate towards $\mathbf{B}_{\mathrm{mag}}+\mathbf{B}_{\mathrm{defl}}$ making the curvature analysis as a function of the applied fields more demanding. The dependence of $\mathbf{T}(\mathbf{B}_{\mathrm{defl}})$ can be used to gain information about the film anisotropy. Whether a magnetic anisotropy has to be considered large or small for exploiting magnetically induced torques for magnetometry can be decided by the following consideration.

The measured deflection of the sample in a cantilever bending magnetometer is rather small. For our setup the deflection at the end of the 7 mm long cantilever with a crystal carrying 10 ML of Fe amounts to only 1 nm at an external field of 6.6 mT, this corresponds to a minute tilt of the sample of only 0.4 μrads. Such small angular changes are easily detected by the optical deflection technique, but do not lead to a considerable change of the orientation of the film magnetization in the external field. Thus, for the discussion of anisotropy effects it is fair to assume that the sample is mounted on an infinitely rigid substrate. Then the magnetically induced torque is given by the partial derivative of the energy density f with respect to the angle ϑ between surface normal $\mathbf{n}$ and magnetization $\mathbf{M}$:

$$f(\vartheta,B_{\mathrm{defl}})=\left[\frac{\mu_0 M^2}{2}\cos^2\vartheta+K_V\cos^2\vartheta\right]+\frac{1}{d}[K_S^{(1)}+K_S^{(2)}]\cos^2\vartheta-[\sin(\vartheta)B_{\mathrm{mag}}+\cos(\vartheta)B_{\mathrm{defl}}]. \quad (2)$$

In Eq. (2) $\mu_0 M^2/2$ is the shape anisotropy, caused by dipolar interactions of the magnetic moments. K_V is the volume anisotropy constant which contains the crystal anisotropy and magnetoelastic anisotropy contributions. $K_S^{(1)}$ and $K_S^{(2)}$ are the anisotropy contributions from the surface of the film and the film–substrate interface. Finally, the last term is the Zeeman energy of the film in the external fields, here oriented as in the geometry of Fig. 1(a). In the absence of external fields the direction of the spontaneous magnetization is determined by the anisotropy terms.

For thick films the shape anisotropy dominates, which prefers an in-plane orientation of the magnetization, which means that the angle of minimum energy is $\vartheta=90°$. To estimate the influence of the deflection field one may compare the energy contributions of the anisotropy terms and the Zeeman term. As an example, from the saturation magnetization of iron $(1.707\times10^6\ \mathrm{A/m})$ (Ref. 14) one finds a shape anisotropy energy of 133 μeV per atom, whereas the Zeeman energy is in the range of $m_{\mathrm{atom}}^{\mathrm{Fe}}B_{\mathrm{defl}}=2.2\mu_B\times10$ mT $=1.3$ μeV per atom, with $\mu_{\mathrm{B}}=9.27\times10^{-24}$ J/T being the Bohr magneton and a typical deflection field of $B_{\mathrm{defl}}=10$ mT. As the Zeeman energy is 2 orders of magnitude smaller than the anisotropy energy, the orientation of the magnetization given by the angle ϑ is hardly influenced by the external field. To derive the magnetically induced torque T, one has to calculate $T=\partial f(\vartheta,B_{\mathrm{defl}})/\partial\vartheta$ and can then replace cos ϑ by 0 and sin ϑ by 1 and finally gets $T=mB_{\mathrm{defl}}$.

In the case of vanishing anisotropy however, the influence of the Zeeman energy will be decisive for the orientation of the magnetization. Any deviation of a proportionality between measured deflection and magnitude of the deflection field indicates a deviation of the direction of magnetization due to the Zeeman energy term.

To check, whether the expression $T=mB_{\mathrm{defl}}$ can be used, one measures the cantilever deflection as a function of the deflecting field. In the case of linear behavior, as in all the examples given below, the deflection field does not influence the direction of magnetization.

III. ANALYSIS OF MAGNETICALLY INDUCED DEFLECTION

To calculate the magnetic moment of the film from a magnetically induced deflection of a cantilever, we have to

Downloaded 20 Mar 2001 to 195.37.184.165. Redistribution subject to AIP copyright, see http://ojps.aip.org/rsio/rsicpyrts.html

know how a cantilever bends under the influence of a torque. Two cases have to be distinguished. (I) (our case): the film is on a compact crystal and the torque acts only at the end of the cantilever. (II) The film is directly evaporated onto the cantilever and the cantilever bends under the influence of a distributed torque. We will treat both cases like the bending of beams[15] as the appropriate expressions have not been applied in previous work. The relation between the second derivative of the deflection $w(x)$ with respect to the position x along the cantilever length and the bending moment $M_b(x)$ is given by[15]

$$\frac{\partial^2 w(x)}{\partial x^2} = \frac{-M_b(x)}{EI_y}. \tag{3}$$

E is Young's modulus of the bending beam and I_y is the areal moment of inertia of the beam (for rectangular cross sections of the beam: $I_y = ba^3/12$, b: width, a: thickness); $x=0$ indicates the free end of the cantilever.

In case (I) the bending moment is $M_b(x) = T$ for any point of the beam. Twice integrating Eq. (3) and considering the boundary conditions (no deflection and no slope at the clamped end) leads to the expression for the bending line

$$w_c(x) = \frac{Tl^2}{2EI_y}\left[1 - \frac{2x}{l} + \left(\frac{x}{l}\right)^2\right] \tag{4}$$

with the length of the cantilever given by l.

In case (II) the torque is distributed along the cantilever and if we suppose the magnetic film to be distributed over the whole length, then in any point of the cantilever only the fraction T/l of the torque acts and the resulting bending moment is $M_b(x) = Tx/l$. Again twice integrating formula (3) and taking the boundary conditions into account, one gets

$$w_d(x) = \frac{Tl^2}{6EI_y}\left[2 - \frac{3x}{l} + \left(\frac{x}{l}\right)^3\right]. \tag{5}$$

Note that this bending line for the *distributed torque* is the same as in the case of a *force* $F = T/l$ acting only at the *end* of the cantilever.

In the case of a film that is evaporated only onto a part of the cantilever starting at the free end, that means in a region $0 \leqslant x < a$, the bending moment is $M_b(x) = T$ for $x < a$ and $M_b = Tx/a$ for $0 \leqslant x < a$. The expression for the resulting beamline is then given as

$$w(x) = \frac{T}{EI_y a}\left[\frac{x^3}{6} + \frac{a^2 x}{2} - alx + \frac{al^2}{2} - \frac{a^3}{6}\right], \quad 0 \leqslant x < a,$$
$$w(x) = \frac{T(l-a)^2}{2EI_y}\left[1 - \frac{2(x-a)}{l-a} + \left(\frac{x-a}{l-a}\right)^2\right], \quad a \leqslant x \leqslant l, \tag{6}$$

with the additional boundary condition, that both parts of Eq. (6) give the same deflection and the same slope at $x = a$. Figure 2 shows the different bending lines according to Eqs. (4)–(6) and their derivatives, calculated for a Si(100) cantilever with the dimensions 5 mm×15 mm×70 μm, which carries a magnetic moment of 2.5×10^{-6} J/T (corresponding to 100 ML Fe in the case of the distributed torque) in an external magnetic field of 6.6 mT.

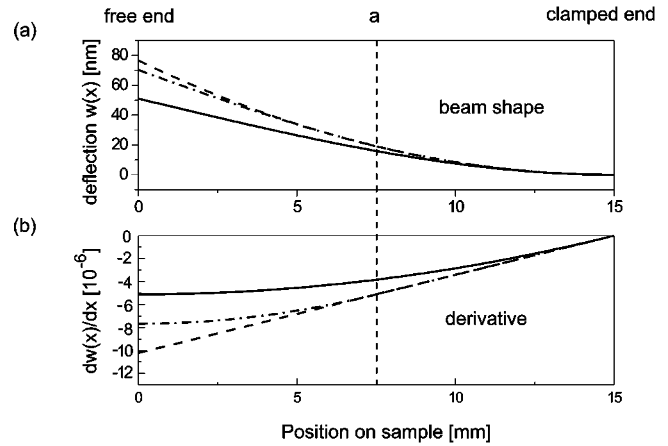

FIG. 2. Calculated deflection curves $w(x)$ of the cantilever (a) and derivatives $\partial w(x)/\partial x$ (b) for a cantilever under the influence of an upward torque acting on the free end (—), a torque distributed along the whole cantilever (- - -), and a torque only acting at $0 < x < a$ (· — · —); a: dashed vertical line. The calculation has been performed for a 5 mm×15 mm×250 μm Si(100) cantilever, see the text.

It is important to realize that in earlier articles[13,16] an incorrect formula for the bending of a cantilever under the influence of a magnetically induced torque has been given. The reason may be that in these articles the problem is treated in a way that is correct for the case of a beam under the influence of a mechanical stress on one of its surfaces. Such surface stresses can be caused, e.g., by a strained film on the cantilever, and would lead to a bending of the cantilever only in the region of the acting stress. However, Eq. (4) clearly shows, that even a torque only acting on the very end of the cantilever leads to deflection at any point of the cantilever.

IV. EXPERIMENT

The magnetometer is part of an UHV chamber shown in Fig. 3 with a base pressure of 5×10^{-11} mbar. In the upper part of the chamber the films are prepared by thermal evaporation at a pressure lower than 5×10^{-10} mbar and can be investigated with AES and LEED. A manipulator with differentially pumped motion feedthrough and a vertical stroke of 60 cm is used to transfer the sample into a glass adapter. This glass adapter is positioned in the crossed magnetic fields of an electromagnet and a pair of deflection coils. The whole chamber with the 600 kg electromagnet is mounted on pneumatic isolators to reduce the influence of mechanical vibrations of the environment on the magnetic measurements.

Figure 4 shows the sampleholder. It consists of a base plate which carries the crystal and a covering plate. Both are made from 50 μm thin molybdenum sheets. The crystal is positioned between the base plate and the covering plate, isolated by additional mica platelets. The base plate acts as the cantilever. The sampleholder base plate is designed such, that a current I can flow around the ring-shaped cutout below the crystal. This current through the circular cutout serves as a calibration coil and produces a magnetic moment $\mathbf{m}$ perpendicular to the crystal surface. A current of 1 mA leads to a magnetic moment of 4.4×10^{-8} J/T, which corresponds to

Downloaded 20 Mar 2001 to 195.37.184.165. Redistribution subject to AIP copyright, see http://ojps.aip.org/rsio/rsicpyrts.html

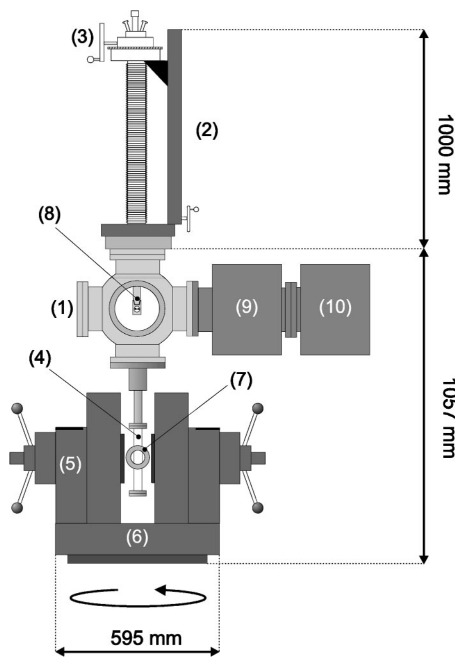

FIG. 3. Schematic of the UHV chamber: The films are prepared by thermal evaporation in the preparation chamber (1) where they are analyzed by AES and LEED. The sample is moved into the magnetic field of an electromagnet (5) and the deflection coils (7) for the magnetic measurements. (1) Preparation chamber, (2) manipulator, (3) differentially pumped rotary motion drive, (4) glass adapter, (5) electromagnet, (6) rotary motion plate, (7) deflection coils, (8) sampleholder with sample, (9) titanium sublimation pump, and (10) ion getter pump.

the magnetic moment of 13 ML Fe covering the crystal used in our experiment. With this electrically induced moment the magnetometer is calibrated *in situ*. An additional small pin on the baseplate touches the crystal from the back side and ensures the grounding of the crystal without shorting the calibration coil.

The bending of the sampleholder caused by the magnetically induced torque is measured by a light beam technique very similar to that used by Sander *et al.*[17] The setup is shown in Fig. 5: A laser and a split photodiode as a position sensitive detector are mounted on one platform. The laserbeam is reflected from the sample to the detector, which is mounted on a piezo translator. The piezo translator is used to obtain the calibration *position signal versus displacement* of the deflection technique. If the sample bends, a position signal will be obtained that is directly proportional to the change of slope of the sample.

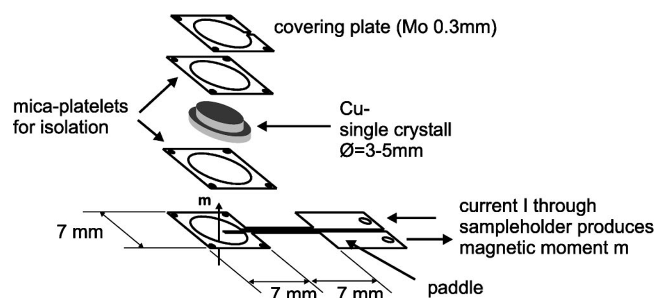

FIG. 4. The crystal is clamped between a sampleholder baseplate and a covering plate, both made from 50 μm molybdenum, isolated by two mica platelets. A current I through the sampleholder produces a magnetic moment perpendicular to the sample surface which is used to calibrate the magnetometer.

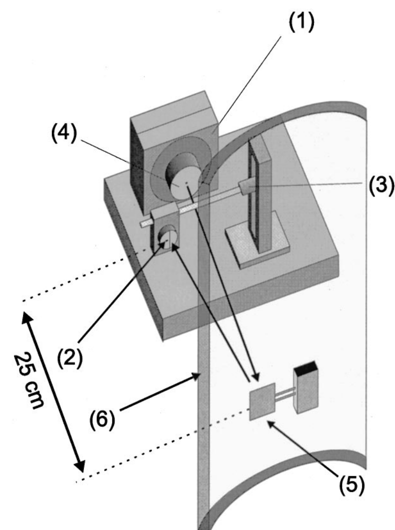

FIG. 5. Schematic of the optical deflection setup. The laser (4) and split photodiode (2) are mounted on one platform. The distance laser (4) to sample (5) is approximately 25 cm. The split photodiode is calibrated by moving the piezo translator (3) by a known amount and detecting the corresponding position signal. (1) Laser gimbal mount, (2) split photodiode, (3) piezo translator, (4) laser, (5) sampleholder with sample, and (6) glass adapter.

To improve the sensitivity of the method all the measurements were performed using an alternating deflection field $\mathbf{B}_{\mathrm{defl}}(t)=\mathbf{B}^0_{\mathrm{defl}}\sin(\omega t)$. This leads to an alternating signal from the split photodiode which is measured by a lock-in amplifier. The alternating deflection field causes eddy currents in the single crystal, which in turn lead to a magnetic moment $\mathbf{m}_{\mathrm{eddy}}$ in the direction of the deflection field. Because the magnetizing field $\mathbf{B}_{\mathrm{mag}}$ is perpendicular to this moment an additional torque $\mathbf{T}_{\mathrm{eddy}}=\mathbf{m}_{\mathrm{eddy}}\times\mathbf{B}_{\mathrm{mag}}$ arises. While the torque $\mathbf{T}=\mathbf{m}\times\mathbf{B}_{\mathrm{defl}}$ reaches its maximum value when the deflection field is at its maximum, the torque $\mathbf{m}_{\mathrm{eddy}}$ has the highest value when the change of the deflection field is maximal. Due to the sinusoidal time dependence of $\mathbf{B}_{\mathrm{defl}}(t)$ this happens exactly, when $\mathbf{B}_{\mathrm{defl}}(t)=0$. The magnetically produced torque $\mathbf{T}$ and the torque $\mathbf{T}_{\mathrm{eddy}}$ caused by the eddy currents are therefore phase shifted by 90°. The eddy current induced torque is proportional to both frequency of the deflection field and magnitude of the magnetizing field. Using typical experimental parameters for the frequency of the deflection field of 10 Hz with an amplitude of 1 mT and a magnetizing field of 10 mT we find that the eddy current signal is as large as the true magnetic signal corresponding to roughly 100 ML. The estimate holds for in-plane magnetized samples, where the alternating deflection field penetrates the large surface area of the substrate. For out-of-plane magnetized samples, the deflection field penetrates the much smaller cross section of the sample, leading to an order of magnitude smaller eddy current signal. However, phase sensitive signal detection with a lock-in amplifier is used to detect the small magnetic signal in the presence of the larger eddy current signal. First, the lock-in amplifier is adjusted to maximize the eddy current signal at a large magnetization field where the total signal is dominated by the eddy current

Downloaded 20 Mar 2001 to 195.37.184.165. Redistribution subject to AIP copyright, see http://ojps.aip.org/rsio/rsicpyrts.html

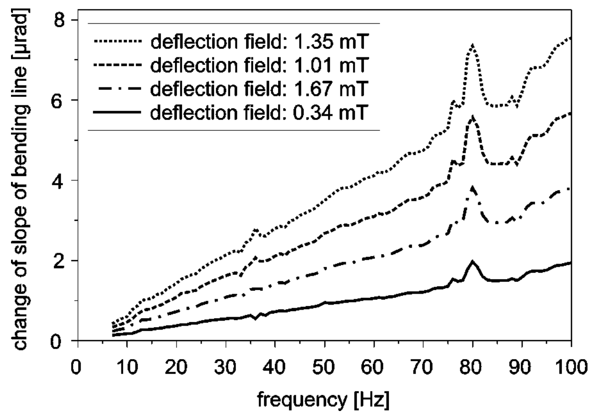

FIG. 6. Frequency dependence of the eddy current induced deflection signal. The amplitude of the signal is proportional to the frequency and the amplitude of the deflection field. The measurements were performed with a Cu single crystal substrate using a 250 μm molybdenum sample holder with a resonance frequency around 200 Hz. The structures in the curves at 36 and 80 Hz are caused by mechanical resonances of the manipulator. Magnetic measurements are performed at 7 Hz.

effect, then the phase is shifted by 90° to measure the true magnetization induced torque.[18] Nevertheless, as the amplitude of the eddy current signal increases linearly with the frequency of the deflection field, see Fig. 6, lower frequencies are preferably used in the experiment. We have chosen 7 Hz for the frequency of the deflection field. This frequency turned out to be a good compromise for having rather low eddy current induced signal contributions but still being above the omnipresent strong mechanical vibrations in the mHz–Hz regime.

The magnitude of the eddy current signal is cumbersome especially for an in-plane magnetized system and can be minimized by using the thinnest metal substrates that are available, or by switching to insulating substrates where feasible. Note however, that a slight misalignment of the phase of the lock-in amplifier is not detrimental as it leads to an eddy current signal proportional to the magnetizing field. As a result, the magnetization curve gets tilted. A horizontal magnetization curve for larger magnetizing fields can be taken as an indication of a properly adjusted phase, for cases where magneto-optical Kerr effect (MOKE) experiments indicate rectangular hysteresis curves.

V. RESULTS

The cantilever magnetometer has been used to measure the magnetization of Fe monolayers on Cu(100). Although the magnetic properties of Fe/Cu(100) have been investigated by many different techniques, e.g., linear[19–22] and nonlinear[23] magneto-optical Kerr effect, ferromagnetic resonance,[24] Mössbauer spectroscopy,[25,26] or magnetic circular dichroism in x-ray absorption spectroscopy[27,28] there are no magnetization data obtained by the application of a *direct* method to this epitaxial system.

Figure 7 shows our cantilever magnetometry results for 23 ML of Fe with a 6.6 mT deflection field at 7 Hz. In this thickness range Fe shows an in-plane easy axis of magnetization.[29] The left panel shows the raw data. The middle panel shows the disturbing effect caused by the manipulator.

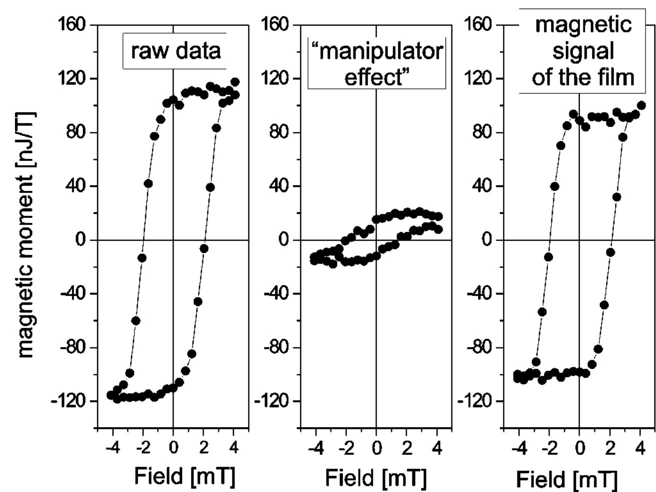

FIG. 7. Measurement of 23 ML Fe on Cu(100). The raw data, left panel, have to be corrected for the disturbing hysteresis-like effect caused by the manipulator shown in the middle panel. The magnetic signal of the film is obtained as the difference between the raw data and the disturbing effect and is shown in the right panel. The total magnetic moment of the film is $9.5 \pm 1 \times 10^{-8}$ J/T, that corresponds to 2.4 ± 0.2 μ_B per atom.

These data have been obtained by performing the same magnetometry measurement with the clean Cu(100) surface. The hysteresis-like shape of the curve originates from the influence of the magnetic fields on the partially magnetic parts of the manipulator. Additional contributions might arise from a contamination of the manipulator with the ferromagnetic film material during deposition. The right panel shows the corrected data, which is the difference between the raw data and the manipulator effect. As the thickness (46.5 Å) and the area (10.7 mm^2) of the film are known one gets from the measured total magnetic moment of $9.5 \pm 1 \times 10^{-8}$ J/T a moment per atom of 2.4 ± 0.2 μ_B.

The measurements have been repeated for films with different thicknesses. The magnetic moment of the films obtained from these hysteresis loops are shown in Fig. 8. The data were fitted by a straight line through the zero point and from the slope of the fitted curve we deduce a magnetic

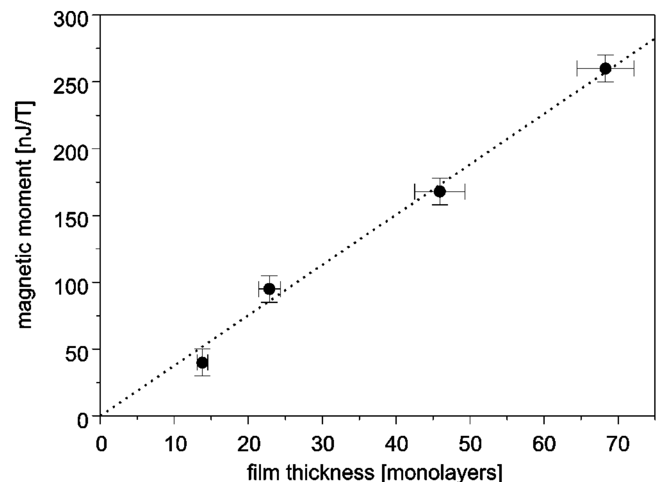

FIG. 8. Magnetic moment of in-plane magnetized Fe/Cu(100) films. From the slope of the fitted curve the magnetic moment per atom of the bcc-monolayer is deduced to be the bulk value of 2.2 ± 0.1 μ_B.

Downloaded 20 Mar 2001 to 195.37.184.165. Redistribution subject to AIP copyright, see http://ojps.aip.org/rsio/rsicpyrts.html

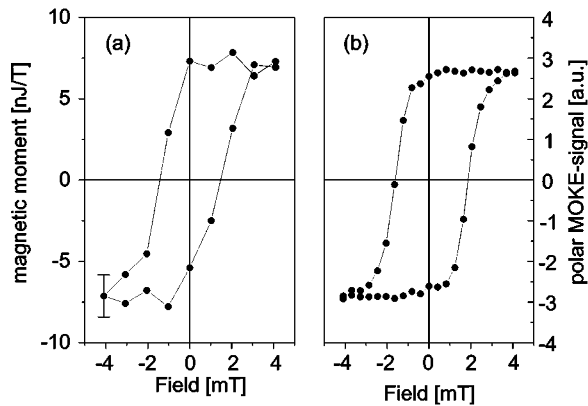

FIG. 9. Hysteresis loop of a 2.5 ML Fe/Cu(100) film. (a) Cantilever magnetometry in ''compensation mode,'' with a deflection field of 6.6 mT at 7 Hz. The film is magnetized perpendicular to the surface and the compensation mode leads to a submonolayer sensitivity with a better signal to noise ratio as compared to the data presented in Fig. 8. (b) Polar MOKE measurement taken *in situ* at the same sample.

moment per atom of 2.2±0.1 μ_B in the investigated thickness range. Within the error this corresponds to the known bulk value of Fe of 2.2 μ_B at 300 K.

In the thickness range below 11 ML Fe/Cu(100) shows an easy axis of magnetization out of plane.[19,20,30,31] In this thickness range we take advantage of the fact that the magnetic moment of the film and moment of the sampleholder are aligned parallel or antiparallel, respectively. By passing a current through the sampleholder one can compensate the polar magnetic moment of the film. At this point the torque arising from the ferromagnetic sample in the external field and the torque produced by the sampleholder add to zero net torque. Figure 9 shows the result of such a zero measurement performed on a 2.5 ML Fe film on Cu(100). The deflection field was the same as in the case of the in-plane magnetized films (6.6 mT, 7 Hz). On the same film an additional measurement of the polar magneto-optical Kerr effect has been performed and is also shown in Fig. 9. From the cantilever magnetometry we get a magnetic moment of the film of $7.0\pm1.3\times10^{-9}$ J/T, which corresponds to a magnetic moment per atom of 1.75 ± 0.3 μ_B.

For such a 2.5 ML Fe film, a groundstate moment of 2.8 μ_B per atom has been predicted in calculations[32,33] and confirmed experimentally by magnetic circular dichroism in x-ray absorption[28] at 110 K. As our measurements have been performed at room temperature, the temperature dependence of the magnetization has to be taken into account. As Detzel *et al.*[34] show, the Curie temperature of such films is reduced to $T_C = 330$ K and the magnetization at room temperature is only about 70% of its value at 0 K. Thus, extrapolating the moment we measured at 300 K down to 0 K our measurement of the magnetic moment gives 2.4±0.4 μ_B and agrees within the error margin with the work mentioned above.

To reduce the error, which is currently mainly caused by the manipulator effect, as discussed above, the partially magnetic parts of the manipulator have to be replaced by other materials. First attempts in this way look very promising.

In conclusion, the cantilever magnetometer is a powerful experimental technique that can be used for magnetometry of monolayers under UHV conditions.

The application of a composite sample holder that employs standard size single crystals mounted on a cantilever is a powerful alternative to the use of thin single crystal substrates for monolayer magnetometry. This extends the application of cantilever magnetometry to cases where thin substrates are not available. Nevertheless, an easy use of thin substrates to enable stress measurements is still possible.

The fact that torque measurements rely upon the existence of ferromagnetic anisotropy is useful in two respects. On the one hand, the absence of anisotropies in the dia- or paramagnetic substrates allows us to measure only the magnetic moment of the ferromagnetic film without having to fight the contribution of the substrate to the magnetic moment. Note that in the worst case the ''clean'' sample volume of 11 mm^3 might induce a paramagnetic or diamagnetic signal corresponding to roughly a tenth of a monolayer at 1 mT magnetizing field, which is presently below our detection limit. On the other hand, the interplay between magnetic anisotropy and Zeeman energy offers the additional possibility to gain information about the anisotropy constants of thin films.

In contrast to the venerable TOM technique, which also uses magnetically induced torques, the magnetizing and the deflecting fields are independent from each other. This allows us to measure the magnetization of the sample in remanence. Beyond that, no additional compensation of the eddy current effect is necessary for the presented cantilever magnetometry.

ACKNOWLEDGMENT

The authors would like to thank U. Gradmann for fruitful discussions, especially concerning the data analysis.

[1] U. Gradmann, in *Handbook of Magnetic Materials*, Vol. 7, edited by K. H. J. Buschow (Elsevier, Amsterdam, 1993), pp. 1–96.
[2] *Ultrathin Magnetic Structures Volumes I+II*, 1st ed., edited by J. A. C. Bland and B. Heinrich (Springer, Berlin, 1994).
[3] R. M. Bozorth and H. J. Williams, Phys. Rev. **103**, 572 (1956).
[4] H. Zijlstra, Rev. Sci. Instrum. **41**, 1241 (1970).
[5] R. T. Lewis, Rev. Sci. Instrum. **47**, 519 (1976).
[6] S. Foner, Rev. Sci. Instrum. **47**, 520 (1976).
[7] S. Foner, IEEE Trans. Magn. **17**, 3558 (1981).
[8] P. J. Flanders, J. Appl. Phys. **63**, 3940 (1988).
[9] R. Bergholz, Ph.D. thesis, Technische Universität Clausthal, 1984.
[10] St. Miethaner, Ph.D. thesis, Universität Regensburg, 1998.
[11] D. P. Pappas, G. A. Prinz, and M. B. Ketchen, Appl. Phys. Lett. **65**, 3401 (1994).
[12] S. Spagna, R. E. Sager, and M. B. Maple, Rev. Sci. Instrum. **66**, 5570 (1995).
[13] M. Weber, R. Koch, and K. H. Rieder, Phys. Rev. Lett. **73**, 1166 (1994).
[14] Ch. Kittel, *Introduction to Solid State Physics*, 7th ed. (Wiley, New York, 1996).
[15] R. J. Roark, *Formulas for Stress and Strain*, 6th ed. (McGraw-Hill, New York, 1989).
[16] D. Sander, A. Enders, and J. Kirschner, IEEE Trans. Magn. **34**, 2015 (1998).
[17] D. Sander, A. Enders, and J. Kirschner, Rev. Sci. Instrum. **66**, 4734 (1995).
[18] Th. Höpfl, Ph.D. thesis, Martin-Luther-Universität Halle Wittenberg, 2000.
[19] C. Liu, E. R. Moog, and S. D. Bader, Phys. Rev. Lett. **60**, 2422 (1988).
[20] P. Xhonneux and E. Courtens, Phys. Rev. B **46**, 556 (1992).

Downloaded 20 Mar 2001 to 195.37.184.165. Redistribution subject to AIP copyright, see http://ojps.aip.org/rsio/rsicpyrts.html

[21] D. Li, M. Freitag, J. Pearson, Z. Q. Qiu, and S. D. Bader, Phys. Rev. Lett. **72**, 3112 (1994).
[22] A. Kirilyuk, J. Giegiel, J. Shen, and J. Kirschner, Phys. Rev. B **54**, 1050 (1996).
[23] M. Straub, R. Vollmer, and J. Kirschner, Phys. Rev. Lett. **77**, 743 (1996).
[24] W. Platow, A. N. Anisimov, M. Farle, and K. Baberschke, Phys. Status Solidi A **173**, 145 (1999).
[25] R. D. Ellerbrock, A. Fuest, A. Schatz, W. Keune, and R. A. Brand, Phys. Rev. Lett. **74**, 3053 (1995).
[26] D. J. Keavney, D. F. Storm, J. W. Freeland, I. L. Grigorov, and J. C. Walker, Phys. Rev. Lett. **74**, 4531 (1995).
[27] J. Dunn, D. Arvanitis, and N. Mårtensson, Phys. Rev. B **54**, R11 157 (1996).
[28] D. Schmitz, C. Charton, A. Scholl, C. Carbone, and W. Eberhardt, Phys. Rev. B **59**, 4327 (1999).
[29] R. Allenspach and A. Bischof, Phys. Rev. Lett. **69**, 3385 (1992).
[30] D. Pescia, M. Stamponi, G. L. Bona, A. Vaterlaus, R. F. Willis, and F. Meier, Phys. Rev. Lett. **58**, 2126 (1987).
[31] M. Stamponi, Appl. Phys. A: Solids Surf. **49**, 449 (1989).
[32] C. L. Fu and A. J. Freeman, Phys. Rev. B **35**, 925 (1987).
[33] V. L. Moruzzi, P. M. Marcus, K. Schwarz, and P. Mohn, Phys. Rev. B **34**, 1784 (1986).
[34] Th. Detzel, M. Vonbank, M. Donath, N. Memmel, and V. Dose, J. Magn. Magn. Mater. **152**, 287 (1996).

Downloaded 20 Mar 2001 to 195.37.184.165. Redistribution subject to AIP copyright, see http://ojps.aip.org/rsio/rsicpyrts.html